First-principles study of the surface energy and work function of III-V semiconductor compounds

W. Liu, W. T. Zheng, and Q. Jiang*
Key Laboratory of Automobile Materials, Ministry of Education, and Department of Materials Science and Engineering, Jilin University, Changchun 130022, China

(Received 12 January 2007; revised manuscript received 18 April 2007; published 22 June 2007)

Surface energy and work function of 12 III-V semiconductors, AlP, AlAs, AlSb, AlBi, GaP, GaAs, GaSb, GaBi, InP, InAs, InSb, and InBi, on (110) surfaces are calculated using *ab initio* density functional theory. The obtained values are proportional to the corresponding cohesive energy and are in good agreement with available experimental data and theoretical models. The linear relationship among cohesive energy, surface energy, and work function is interpreted by analyzing their electronic properties where four (110) surfaces of Al series semiconductors, AlP, AlAs, AlSb, and AlBi, are taken as examples.

DOI: 10.1103/PhysRevB.75.235322 PACS number(s): 68.47.Fg, 05.70.Np, 73.30.+y, 31.15.Ar

I. INTRODUCTION

The surfaces of III-V semiconductor compounds are of vital importance because the functioning of modern electronic devices is strongly influenced by their cleanliness, geometries, and photoelectric properties.[1,2] As what Kroemer stated, the winner of the 2000 Nobel Prize, "by increasing miniaturization in semiconductor-device technology, the interface itself is the device."[3] Among different surface orientations, the nonpolar III-V(110) surface is the most widely studied, especially concentrated on its relaxed geometry,[2,4–6] phonon vibration,[6–9] and band structure.[2,10,11] The corresponding surface energy γ and work function Φ are two essential parameters to fully characterize the surface.[11,12] In previous work, γ has been utilized to discuss the morphology changes of GaAs and InAs surfaces[13] and the "crack-healing" phenomenon in a GaP(110)/GaAs(110) system.[14] On the other hand, the Φ values are often used to judge the flowing direction of charges for a metal-semiconductor interface.[15] Nowadays, highly mismatched III-V surfaces are under development for a number of applications in thin-film devices.[14] Since the thin-film process technology is intimately related to fundamental investigations in surface and interface,[16] their basic parameters including γ and Φ should be accurately determined firstly. However, despite their broad applications, scarce values of III-V(110) surfaces are reported because of their difficulties in measurements.[17–19]

γ is defined as the difference between the free energy of a surface atom and that of an interior one for a solid, which is one of the basic qualities to describe the surface stabilities.[20] In most experiments, it is obtained by extrapolating the surface energy values of the liquid at high temperatures.[17] This leads to very less reliable experimental data for compounds.[21] In our knowledge, merely one experimental work[22] and three theoretical works[23–25] have reported the γ values of III-V(110) surfaces. In 1981, Messmer and Bilello[22] measured the GaAs(110) and GaP(110) surfaces using a modified spark discharge method, and obtained $\gamma_{GaAs}=0.61\pm0.11$ eV/atom and $\gamma_{GaP}=1.23\pm0.13$ eV/atom. The above data are somewhat unsatisfactory due to their larger error bars. In addition, $\gamma_{GaAs} \ll \gamma_{GaP}$ is nearly impossible, since the cohesive energy E_c of GaAs is only 9.86% lower than that of GaP (it seems that the γ_{GaAs} value is more correct). In the aspect of theoretical calculations, Qian *et al.*[23] firstly simulated the GaAs(110) surface using the local density approximation (LDA) functional with the Ceperley-Alder-Perdew-Zunger (CAPZ) method.[26,27] Their result of $\gamma_{GaAs}=0.61$ eV/atom is in excellent agreement with the experimental value. After that, Moll *et al.*[24] and Zhang and Wei[25] recalculated γ_{GaAs} with essentially the same LDA functional, and also obtained accurate results compared with experiments. These, in turn, proved the good performance of LDA functional in surface calculations.[28]

In fact, the γ values of pure elements[18,29,30] and other compounds[31,32] have also been calculated using density functional theory (DFT) method. In our earlier work, the transition metal carbides (TMCs), transition metal nitrides (TMN), and alkaline metal oxides (AMOs) have been systemically determine.[12] However, a complete study on the III-V(110) surfaces is still lacking.

Φ was firstly proposed by Einstein in his work on the photoelectric effect, which is defined as the minimum work required to remove a free electron from the interior of a solid to infinitely far away in vacuum.[33] In experiments, Kelvin probe is the most suitable tool to measure Φ values, which measures the contact potential difference between a surface under investigation and a standardized surface.[33,34] Although this method is simple and nondestructive, Φ is very sensitive to the presence of impurities, roughness, and even slight misorientation on the surfaces.[19,33,35] In addition, some other factors can also lower its accuracy, e.g., the sample is not a single crystal but a polycrystal, or the ultrahigh vacuum cannot be ensured.[18] Between 1965 and 1967, Φ values of AlSb,[36] GaP,[37] GaAs,[38] GaSb,[38] InP,[39] InAs,[38] and InSb (Ref. 38) have been systematically measured using Kelvin contact potential difference method. In the aspect of simulations, no Φ values of (110) surfaces of III-V compounds have been carried out, although those of pure metals,[18,30,40] TMCs,[31,41,42] and TMNs[43] have been systemically calculated.

In this contribution, DFT calculations are employed to determine γ and Φ values of cubic III-V(110) surfaces, including the Al series (AlP, AlAs, AlSb, AlBi), Ga series (GaP, GaAs, GaSb, GaBi), and In series (InP, InAs, InSb, InBi). It is found that both γ and Φ values have the same trend with the corresponding E_c values. In addition, our results are in agreement with available experimental and other theoretical results.

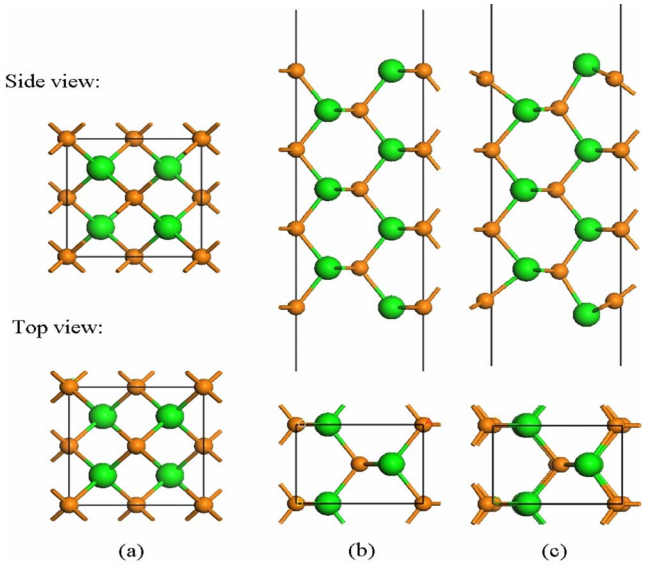

FIG. 1. (Color online) Schematic plots of III-V semiconductor compounds: (a) bulk structure, (b) unrelaxed (110) surface, and (c) fully relaxed (110) surface. The larger sphere shows an anion, while the smaller one shows a cation.

II. CALCULATIONS

All DFT calculations in the Cambridge sequential total energy package (CASTEP) code are employed.[44] Plane-wave ultrasoft pseudopotentials are utilized to render the computations tractable as well as to enhance efficiency.[45] To cleave III-V(110) slabs, bulk compounds should be built and checked firstly in our computer. As we all know, cubic III-V semiconductor compounds are zinc-blende (ZB) structure, with four cations (Al, Ga, In) and four anions (P, As, Sb, Bi) in a unit cell [see Fig. 1(a)]. For bulk calculations, the kinetic cutoff energy and the k points are set to 350 eV and $4\times4\times4$, respectively. In addition, both LDA-CAPZ and generalized gradient approximation (GGA) functional with the PW91 method[46] are employed. After geometry optimization, bulk lattice constant a and E_c are obtained and listed in Table I, from which our results are in excellent agreement with previous reported data.[47–50]

All III-V(110) slabs are created based on the above optimized bulk geometries. Each surface unit cell consists of one cation and one anion with two broken bonds, as shown in Fig. 1(b). No surface reconstruction was detected, although surface relaxation is inevitable.[1,51] The atoms in the middle layer of the slab were constrained, while other layers were allowed to fully relax. After relaxation, the cations move inward while the anions outward [see Fig. 1(c)] because of the charge transfer from the former to the latter.[1,11,24] For surface calculations, the cutoff energy is set to 350 eV and the k points are $4\times4\times4$. Based on these accuracy settings, the convergence tolerance of energy, maximum force, and maximum displacement become 2.0×10^{-5} eV/atom, 0.05 eV/Å, and 2.0×10^{-3} Å, respectively. To avoid the interaction between repeated slabs, a uniform vacuum width of 12 Å is employed.

Note that although GGA is more complex and indeed gives better bulk properties than LDA, "it is well-known that LDA works better than GGA for certain classes of systems and properties, in particular for calculating surface energies and properties of many oxides."[52] This is because LDA shows a better cancellation of errors between surface exchange and correlation energies, which gives slight lower γ

TABLE I. Comparison of the ground state parameters of bulk III-V semiconductor compounds obtained using LDA (a_1,E_{c1}), GGA (a_2,E_{c2}), cited theoretical results (a_3) (Ref. 47), and experimental results (a_4,E_{c3}) (Refs. 48–50). a is the lattice constant in Å, and E_c indicates the cohesive energy in eV/atom, the corresponding electronic structures (metallic or nonmetallic) determined by band structures.

		a_1	a_2	a_3[a]	a_4[b]	E_{c1}	E_{c2}	E_{c3}[c]
AlP	Nonmetallic	5.44	5.45	5.42	5.46	4.90	4.16	
AlAs	Nonmetallic	5.62	5.64	5.61	5.66	4.59	3.78	3.60
AlSb	Nonmetallic	6.09	6.14	6.09	6.14	4.15	3.54	
AlBi	Nonmetallic	6.26	6.41	6.27		3.90	3.14	
GaP	Nonmetallic	5.42	5.51	5.32	5.45	4.45	3.65	
GaAs	Nonmetallic	5.63	5.78	5.53	5.65	4.18	3.29	3.26
GaSb	Nonmetallic	6.04	6.14	5.98	6.09	3.85	3.13	
GaBi	Metallic[d]	6.19	6.29	6.18	6.33	3.64	2.77	
InP	Nonmetallic	5.92	6.03	5.73	5.86	4.14	3.46	3.48
InAs	Nonmetallic	6.11	6.23	5.92	6.05	3.96	3.19	3.10
InSb	Nonmetallic	6.55	6.63	6.35	6.47	3.69	2.88	2.80
InBi	Metallic[d]	6.66	6.80	6.53		3.30	2.71	

[a] a_3 values are obtained by DFT plane-wave pseudopotential method based on LDA functional (Ref. 47).
[b] a_4 values are experimental results (Ref. 48), where GaBi is cited from Ref. 50.
[c] E_{c3} values are experimental results (Ref. 49).
[d] In terms of the band structures, HOMO and LUMO overlap slightly for GaBi and InBi, which indicates that they are not the typical semiconductors, but the metallic or "semimetallic" compounds (Ref. 10).

values than "exact" γ values, while GGA gives much lower and less accurate ones.[53] Therefore, LDA is solely selected as the exchange-correlation functional for γ calculations here. γ is determined as follows[54]:

$$\gamma = [E_{\text{slab}}(N) - NE_{\text{bulk}}]/2, \quad (1)$$

where $E_{\text{slab}}(N)$ is the total energy of an N-layer slab calculated with a sufficient large value of N, E_{bulk} denotes the bulk energy, and "2" in the denominator indicates that two surfaces are involved in the calculations due to three-dimensional boundary conditions. The E_{bulk} values are determined by the slope of the $E_{\text{slab}}(N)$ values versus $N=3$, 5, 7 using the method proposed by Boettger.[54] The calculation is similar to that of our previous work for the γ values of several ceramics, including the TMCs, TMNs, and AMOs.[12]

On the other side, the traditional broken-bond model is again suggested to estimate the γ values. In our previous work, a modified formula was developed,[17]

$$\gamma = [2 - Z_S/Z_B - (Z_S/Z_B)^{1/2}]E_c/2, \quad (2)$$

where Z_S and Z_B denote the coordination number of surface atoms and the corresponding bulk ones, respectively. The model, due to its generality based on bond broken rule, should also be applicable for semiconductor compounds. For ZB structure compounds, it is easy to determine that $Z_S=3$ and $Z_B=4$. For the value of E_c in Eq. (2), the corresponding experimental values E_{c3} should be utilized. However, E_{c3} values of the considered compounds are incomplete and cannot be fully found in literature. Thus, to unify our calculation, simulation results E_{c2} are taken. Note that although the simulation results are used, their correctness has been confirmed by comparing with the known experimental data as seen in Table I.

Φ is determined as an energy difference between a vacuum level E_{vac} and the Fermi energy E_F, which can be expressed as[35]

$$\Phi = E_{\text{vac}} - E_f. \quad (3)$$

In the CASTEP code, the potential energy is imported by clicking on the "Potentials" button in the "Analysis" toolbar. By use of the "Color Maps" tool, the specific value of any position in the slab can be obtained. Obviously, E_{vac} is just the potential value at the center of the vacuum. We remind that every simulation code has its own way of setting E_{vac} and E_F where a relative difference, not an absolute value, is more significant in electronic structure calculations.[11,43] As we all know, E_F is defined as the energy at which half of the possible energy levels in the band are occupied by electrons in terms of the Fermi-Dirac statistics,[55] which is impossible to correctly determine for the nonmetallic systems in DFT-LDA or GGA. Generally, the valence band maximum (VBM) is calculated and selected as a reference for band calculations (for example, the conduction band minimum is obtained by adding the experimental band gap value of E_g to the VBM value).[56,57] In light of this consideration, the Fermi level is simply defined as the VBM for semiconductors and insulators in the CASTEP code and some other codes,[2] which is correct for GaP and GaAs. However, there indeed exists an error in the estimation since $E_F >$ VBM. An alternative is to take $E_F = E_{\text{VBM}} + (1/2)E_g$, which is correct for InSb, but smaller than that for InAs and larger than that for GaP and GaAs.[58] Note that both settings for E_F do not lead to large error since E_g values of the most III-V semiconductors are relatively small, and are even much smaller for III-V(110) surfaces. Thus, the approximation $E_F \approx E_{\text{VBM}}$ is acceptable with evident advantage in simulation since no experimental result is needed to refer. Therefore, $E_F \approx E_{\text{VBM}}$ is taken in our simulation. As a result, the obtained Φ values in Eq. (3) are, in fact, the upper limits of Φ values, or ionization energy I. Note that $(I-\Phi)/I$ is quite small. As an estimation, this value is 6.90% for AlSb(110) surface, which should be an approximate error range in our calculation for Φ.[36]

To choose the exchange-correlation functional, Φ values of GaAs(110) surfaces are calculated using both GGA and LDA. The results show that $\Phi_{\text{GaAs}}=4.78$ eV from LDA is in excellent agreement with the experimental datum of $\Phi_{\text{GaAs}}=4.71\pm0.05$ eV from,[38] while $\Phi_{\text{GaAs}}=5.44$ ev from GGA is 15.50% larger than the experimental result. Thus, LDA-CAPZ function is employed for Φ determinations all through the paper. To ensure the accuracy of our calculations, the vacuum thickness is enlarged from 12 to 20 Å, the slab number is increased from 7 to 11 layers, and the Φ values are converged within 0.05 eV.

III. RESULTS AND DISCUSSION

Table I compares our results of bulk parameters with those from other simulations[47] and experiments.[48–50] For a, both the calculated a_1 and a_2 values respectively from LDA and GGA agree nicely with the experimental results a_4. a_1 is quite close to a_3 since the same LDA functional is employed.[47] For E_c, the differences between LDA results of E_{c1} and GGA results of E_{c2} are obvious. If the experimental results of E_{c3} are chosen as references, E_{c1} are even 26.84% larger, while E_{c2} are merely 2.22% larger than E_{c3} on average. Thus, GGA is far better than LDA in E_c calculations. Comparing LDA and GGA results, the former always gives lower a and larger E_c values than the latter due to the "overbinding" of the latter.[28] Note that the highest occupied molecular orbital (HOMO) and the lowest unoccupied molecular orbital (LUMO) of GaBi and InBi overlap slightly in light of their band structures. Thus, they, in fact, have not been typical semiconductors, but are metallic (or "semimetallic") compounds.[10]

The trends of E_c with four anions of P, As, Sb, and Bi are shown in Fig. 2, which are divided into three series of Al, Ga, and In from top to bottom. In Fig. 2, E_c decreases regularly from left to right if the cations are the same, e.g., $E_{c\text{GaP}} > E_{c\text{GaAs}} > E_{c\text{GaSb}} > E_{c\text{GaBi}}$. In addition, they decrease in sequence for the same anion, e.g., $E_{c\text{AlBi}} > E_{c\text{GaBi}} > E_{c\text{InBi}}$. This is because stronger bonds are built when cations and anions are combined as their electronegativity differences become larger. Therefore, $E_{c\text{AlP}}=4.16$ eV/atom and $E_{c\text{InBi}}=2.17$ eV/atom are, respectively, the largest and smallest values among the 12 compounds.

Table II gives the present γ_1 values from LDA-CAPZ functional and γ_2 values in terms of Eq. (2), where E_c values in Eq. (2) are our GGA simulation results. The corresponding

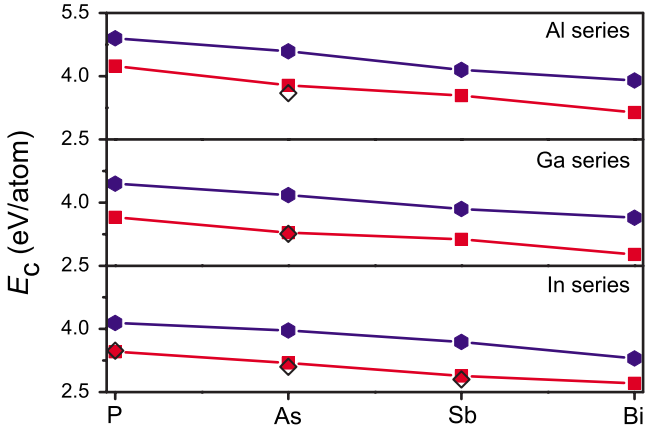

FIG. 2. (Color online) Comparison of E_c values of III-V compounds among simulation results using LDA (E_{c1}), GGA (E_{c2}), and cited simulation results (E_{c3}) (Ref. 49). The symbols ◆, ■, and ◇ denote E_{c1}, E_{c2}, and E_{c3}, respectively.

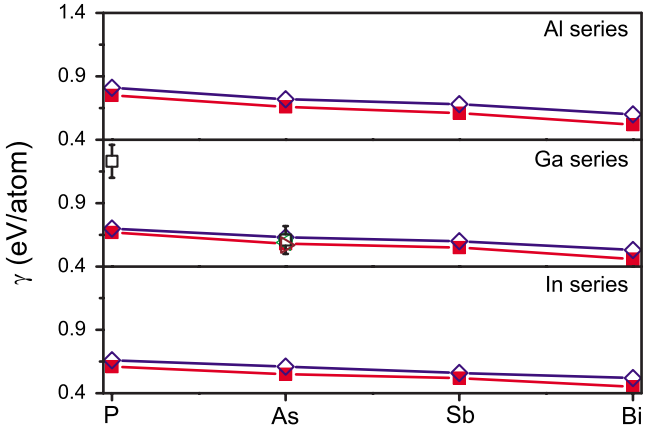

FIG. 3. (Color online) Comparison of γ values of III-V(110) surfaces among simulation results using LDA (γ_1), Eq. (2) (γ_2), cited simulation results (γ_3) (Refs. 6, 23, and 24), and available experimental results (γ_4). The symbols ■, and ◇, and □ denote γ_1, γ_2, and γ_4, respectively, and ○, ▷, and ◁ denote γ_3.

surface electronic structures of III-V(110) are also shown. The cited theoretical data γ_3 (Ref. 23–25) and limited experimental ones γ_4 (Ref. 22) are also shown for comparison purpose. For the GaAs(110) surface, our values of γ_1 =0.58 eV/atom and γ_2=0.63 eV/atom consist with experimental value of γ_4=0.61±0.11 eV/atom,[22] and also correspond with all cited simulation results.[23–25] Thus, Eq. (2) indeed has good performance in determining the γ values of ZB structure compounds because the effect of surface relaxation in Eq. (2) has well been considered, which affects γ values.[17] This is also the case of γ_1 from LDA. Therefore, $\gamma_1 \approx \gamma_2 \approx \gamma_4$.

TABLE II. Comparison of γ values of III-V(110) surfaces in eV/atom among our simulation results γ_1 using LDA-CAPZ, γ_2 based on Eq. (2), other theoretical results γ_3 (Refs. 23–25), and the available experimental results γ_4 (Ref. 22), the corresponding electronic structures (metallic or nonmetallic) determined by band structures.

		γ_1	γ_2	γ_3	γ_4[a]
AlP	Nonmetallic	0.75	0.79		
AlAs	Nonmetallic	0.66	0.72		
AlSb	Nonmetallic	0.61	0.68		
AlBi	Metallic	0.52	0.60		
GaP	Nonmetallic	0.67	0.70	0.61[b]	1.23±0.13
GaAs	Nonmetallic	0.58	0.63	0.59[c] 0.57[d]	0.61±0.11
GaSb	Nonmetallic	0.55	0.60		
GaBi	Metallic	0.46	0.53		
InP	Nonmetallic	0.61	0.66		
InAs	Nonmetallic	0.55	0.61		
InSb	Nonmetallic	0.52	0.56		
InBi	Metallic	0.45	0.52		

[a]Reference 22.
[b]Reference 23.
[c]Reference 24.
[d]Reference 25.

In addition, AlBi, GaBi, and InBi (110) surfaces are metallic, in which an insulator-metal transition of AlBi on (110) surface is present. This is because E_g of a surface narrows in comparison with the corresponding bulk value, and this change even leads to an insulator-metal transition when the corresponding bulk E_g value is small. Note that the bulk GaBi and InBi are also metallic, while their surfaces have stronger metallic characteristics.

However, our results of GaP(110) largely differ with those from experiments, where γ_1=0.67 eV/atom and γ_2 =0.70 eV/atom are about 45.53% and 43.09% lower than γ_4=1.23±0.13 eV/atom, respectively.[22] In previous work, a lot of researches have proved that γ is proportional to E_c.[12,17] Since $E_{c\mathrm{GaP}}$=3.65 eV/atom and $E_{c\mathrm{GaAs}}$=3.29 eV/atom, then $E_{c\mathrm{GaP}}/E_{c\mathrm{GaAs}}$=1.11, which implies that the ratio of γ_{GaP} and γ_{GaAs} should roughly equal to 1.11. Based on the data in Table I, $\gamma_{\mathrm{GaP}}/\gamma_{\mathrm{GaAs}}$=2.02 from experiments and $\gamma_{\mathrm{GaP}}/\gamma_{\mathrm{GaAs}}$ =1.16 from our LDA calculations. Therefore, one can conclude that our results are more reliable. This difference may be induced by measuring accuracy in experiments where crack length determination and the presence of slight bending moments during tensile loading led to the larger uncertainty of the result.[22]

From Table II, our LDA results are in agreement with those from the modified broken-bond model. In fact, if γ_2 are selected as references, γ_1 are about 9.07% lower on average. Although the absolute values are somewhat different, the same orders can always be found from different methods, as shown in Fig. 3. In every series, γ values decrease along the sequence going from P to Bi. After bond cutting, the energy loss of AlP(110) is the largest, while that of InBi(110) is the smallest. This proves again that the variations of γ are consistent with the corresponding E_c values. The ratios of γ and E_c should be a constant here because all the compounds have the same structure and orientation. In terms of our simulation results in Tables I and II, γ_1/E_{c2} values ranging from 0.17 to 0.18 are very close to γ_2/E_{c2}=0.19 from Eq. (2).

Present simulated results of the relaxed surface Φ_1 and unrelaxed ideal surface Φ_2 and available experimental results

TABLE III. Comparison of Φ values of III-V(110) surfaces in eV between our simulation results using LDA-CAPZ functional relaxed surfaces Φ_1, unrelaxed ideal surfaces Φ_2, and available experimental data Φ_3 (Refs. 36–39). E_{vac} and E_F in eV show the corresponding energies of vacuum level and Fermi level.

	E_{vac1}	E_{F1}	Φ_1	E_{vac2}	E_{F2}	Φ_2	Φ_3[a]
AlP	6.45	1.50	4.95	5.85	1.30	4.55	
AlAs	3.94	−0.80	4.74	3.57	−0.96	4.53	
AlSb	0.28	−4.42	4.70	0.23	−4.42	4.65	4.86±0.05
AlBi	−4.99	−9.49	4.50	−4.88	−9.32	4.44	
GaP	5.68	0.75	4.93	5.73	0.79	4.94	>1.30±0.10[b]
GaAs	3.61	−1.17	4.78	3.36	−1.39	4.75	4.71±0.05
GaSb	−0.02	−4.72	4.70	−0.09	−4.77	4.68	4.76±0.05
GaBi	−5.38	−9.86	4.48	−5.18	−9.76	4.58	
InP	3.07	−1.73	4.80	2.90	−1.71	4.61	4.65±0.10
InAs	1.19	−3.49	4.68	1.07	−3.48	4.55	4.90±0.05
InSb	−1.67	−6.27	4.60	−1.74	−6.25	4.51	4.77±0.05
InBi	−6.52	−10.84	4.32	−6.11	−10.47	4.36	

[a]Φ_3 data are obtained directly from the Kelvin contact potential difference experiments, where GaAs, GaSb, InAs, and InSb are cited from Ref. 38 and AlSb and InP are cited from Refs. 36 and 39, respectively.
[b]1.30±0.10 eV is the lowest achievable Φ value for GaP where there exist some cesium on the prepared surfaces (Ref. 37).

of Φ_3 are shown in Table III. The determined E_{vac} and E_F values in Eq. (3) are also listed. Good agreement can be found between Φ_1 and Φ_3. In fact, if the experimental results are taken as references, Φ_{AlSb}, Φ_{GaSb}, Φ_{InAs}, and Φ_{InSb} are about 3.29%, 1.26%, 4.90%, and 3.56% lower, while Φ_{GaAs} and Φ_{InP} are 1.49% and 3.23% larger than those of Φ_3. This is because DFT calculations typically give the Φ values within 0.1–0.2 eV of the experimental values.[59] Hence, LDA functional has excellent performance in Φ calculations. Note that since there are some Cs on the prepared surface of GaP(110) in the experiments, the corresponding Φ_3 value is smaller than the true one, which should be the reason why $\Phi_3 < \Phi_1$.[37] In addition, the averaged value of $\Phi_1/E_{c2}=1.43$ from our simulation results agrees with $\Phi_3/E_{c2}=1.48$ from available experiments.[36–39] Since the Φ value depends on the charge density in the surface region and varies with energy around,[51,60] the Φ value of a relaxed surface may be larger or smaller than those for an unrelaxed surface, as shown in Table III. The variation of Φ values after the relaxation could be proportional to changes of E_{vac} (surface dipole), i.e., $\Phi_1 > \Phi_2$ when $E_{vac1} > E_{vac2}$ and vice versa. Similar results have been found for TMN surfaces.[43]

Although the absolute values are quite close, Φ_1 and Φ_3 have different trends. From Fig. 4, it is surprising to find that our calculated Φ_1 values also have the same orders of E_c and γ, which has not been reported before in our knowledge. Note that at first glance, it seems that the variation trend of Φ values as a function of composition of compounds in the concerned systems could not be easily determined by their difference in terms of Eq. (3) since both E_{vac} and E_F monotonically decrease. However, the drop of E_{vac} values is indeed more rapid than that of E_F values in these compound systems, which results in that Φ values also decrease monotonically along the sequence going from P to Bi. For Al-based compounds as an example, the difference of E_{vac1} between AlAs and AlP is −2.51 eV, while that of E_{F1} between them is −2.30 eV. As a result, $\Phi_{AlAs} < \Phi_{AlP}$, as seen in Table III. However, the experimental data are disordered, e.g., $\Phi_{GaAs} < \Phi_{GaSb}$ and $\Phi_{InP} < \Phi_{InAs}$. As we all know, III-V compounds are covalently bonded, and the electrons in the outer *s* and *p* orbitals are rigidly bound to the atom; therefore, it is "harder" for an electron to emit from the solid if the binding is stronger.

In fact, previous works have implied (although not stated explicitly) the relationships among Φ, γ, and E_c. For example, linear muffin-tin orbital method has found that Φ and γ roughly have the same trends for 40 elemental metals, including alkali, alkaline earth, divalent rare earth, 3*d*, 4*d*, and 5*d* transition, and noble metals.[18] In addition, for TMC and TMN, the orders of $\Phi_{TiC} < \Phi_{ZrC} < \Phi_{NbC} < \Phi_{TaC} < \Phi_{HfC}$

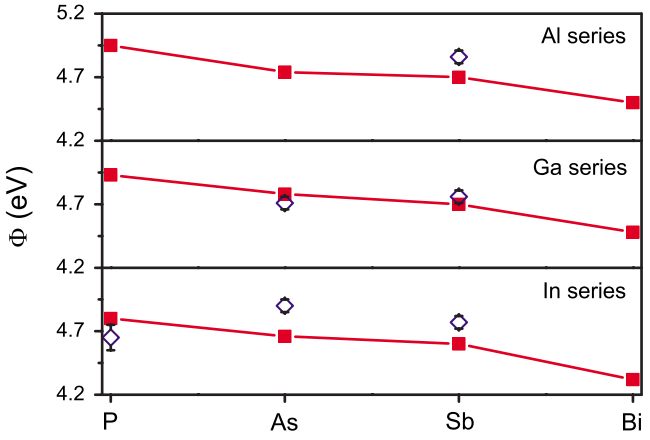

FIG. 4. (Color online) Comparison of Φ values of III-V(110) between simulation results using LDA (Φ_1) and available experimental results (Φ_3) (Refs. 36–39). The symbols ■ and ◇ denote Φ_1 and Φ_3, respectively.

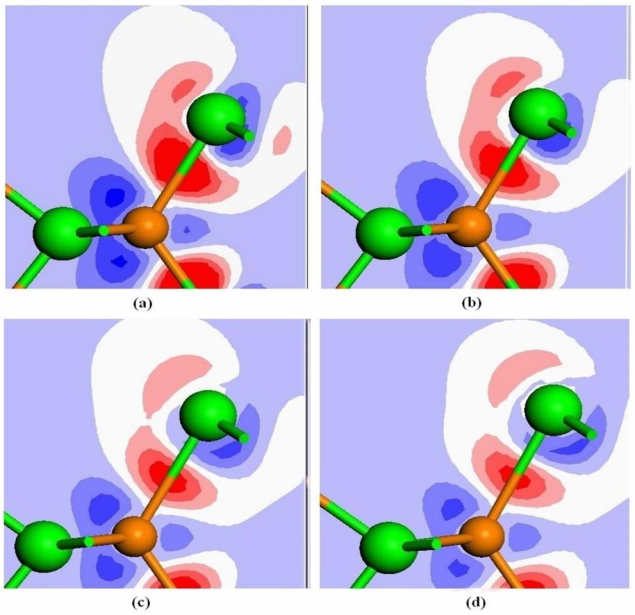

FIG. 5. (Color online) The plots of the electron density difference for the Al series taken along the (110) plane: (a) AlP, (b) AlAs, (c) AlSb, and (d) AlBi. The red region shows the electron accumulation, while the blue region shows the electron loss. The larger sphere shows an anion, while the smaller one shows a cation.

and $\Phi_{TiN} < \Phi_{ZrN} < \Phi_{HfN} < \Phi_{NbN} < \Phi_{TaN}$ from experiments[43] are roughly consistent with those of E_c.[12] For BN(110) surface, both Φ_{BN} and E_{cBN} values are about 60% larger than Φ_{AlP} and E_{cAlP} shown above.[11] The above facts confirm $\Phi \propto E_c$.

To understand the above orders and the bonding nature, the plots of electron density difference for (110) surfaces of Al series (AlP, AlAs, AlSb, and AlBi) are introduced in Fig. 5. In this figure, red and blue regions indicate electron accumulation and loss, respectively. Also in this figure, both cations and anions contribute some charges of their own (the blue regions) and share with each other, since charges mainly accumulate in the middle of a bond. Therefore, III-V(110) slabs are typical covalent slabs. However, although the covalent bonding is predominant, there exists small amount of ionic bonding. As shown in this figure, red regions can also be detected on the top left corner of an anion.

Although the four plots are quite similar, three changes can be found. Firstly, the areas of the red region decrease largely from Fig. 5(a) to Fig. 5(d) in turn. As we all know, the denser the electrons around two atoms, the larger the bonding strength. Thus, the AlP(110) has the strongest bonds, while the AlBi(110) has the weakest bonds in terms of the figure. Secondly, the centers of the red regions move away from the anions from Fig. 5(a) to Fig. 5(d). This is because AlP(110) is most polarized among the four slabs. The above phenomenon is supported by the data from Mulliken analysis, where the charge of Al is increased from 0 to +0.76, +0.45, +0.17, and +0.12 in AlP, AlAs, AlSb, and AlBi, respectively. Finally, we can see the bond length order of AlP < AlAs < AlSb < AlBi.

To further look into the conditions of orbital hybridization, the density of states (DOS) plots of AlP(110) and bulk AlP are determined as examples (see Fig. 6). The AlP(110) surface is a typical semiconductor, since the number of energy states is about zero at E_f, while E_g is within 5 eV. All four plots show three groups of peaks, where the lowest band ranging from −12 to −8 eV corresponds to the core states, the next fully occupied band from −6 to 0 eV is the valence band, and the highest band above 0 eV is the conduction band. From Fig. 6(a), it is found that Al 3s and Al 3p orbitals mix strongly to form sp^3 hybridization orbitals. After that, a P atom fills its five valence electrons into the empty sp^3 orbitals to make them fully filled. As shown in Fig. 6(b), the main peaks of P 3s and P 3p located at −8.98 and −0.43 eV interact with the hybridized Al 3s and Al 3p orbitals. From Figs. 6(c) and 6(d), the DOS plots of bulk AlP are similar to

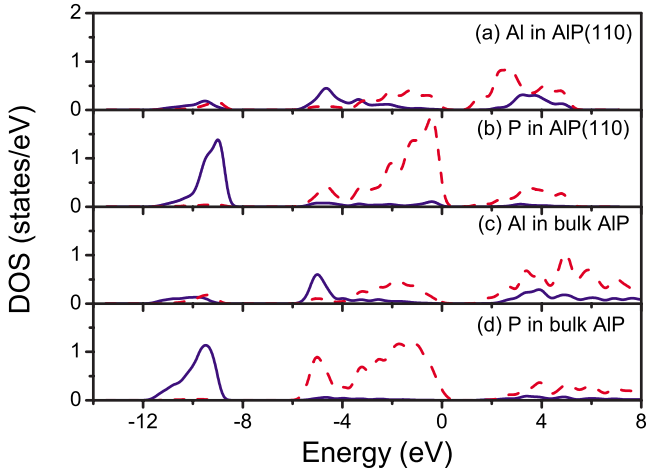

FIG. 6. (Color online) The DOS plots for AlP(110) surface and bulk AlP: (a) Al atom in AlP(110), (b) P atom in AlP(110), (c) Al atom in bulk AlP, and (d) P atom in bulk AlP. The solid and dashed lines indicate the states of s and p, respectively. The Fermi level is located at 0 eV.

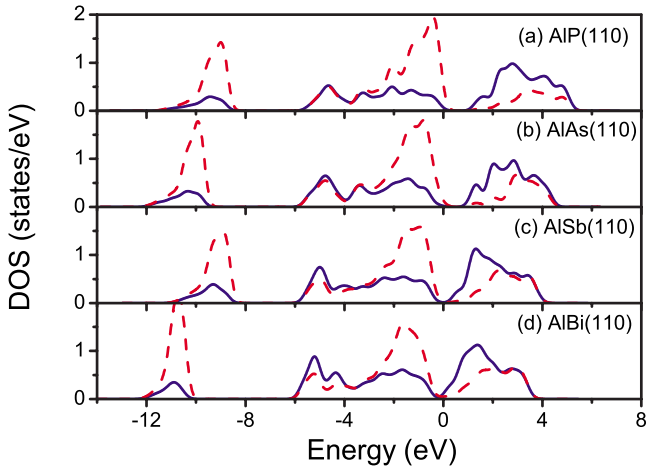

FIG. 7. (Color online) The DOS plots for (110) surfaces of Al series: (a) AlP(110), (b) AlAs(110), (c) AlSb(110), and (d) AlBi(110). The solid and dashed lines indicate the states of an Al atom and an anion (P, As, Sb, or Bi), respectively. The Fermi level is located at 0 eV.

those of the clean surface, but all peaks are moved left. Thus, the clean AlP(110) surface is more active than the bulk. In addition, DOS of AlP(110) surface shows $E_g > 0$ although it is narrower than that of bulk AlP. Since HOMO and LUMO do not overlap in light of the band structure, AlP(110) surface is still nonmetallic.

For comparison purpose, four DOS plots of Al series are shown in Fig. 7. By interacting with each other, all the valence electrons in the cubic take up the empty orbitals in terms of the "eight-minus-n rule," where n is the number of s and p electrons of the atom in question. The main peaks in the energy range of −6–0 eV (valence bands) are shifted left from Fig. 7(a) to Fig. 7(d) in turn. Therefore, AlP(110) is the most active, while AlBi(110) is the most inert surface. Since the γ values increase with the activity of surfaces, their orders can also be interpreted through the DOS plots. In this figure, $E_{g\mathrm{AlP}} > E_{g\mathrm{AlAs}} > E_{g\mathrm{AlSb}} > E_{g\mathrm{AlBi}}$ where insulation properties drop along the series.

Obviously, the above discussions about the electronic properties are suitable for (110) surfaces of GaP, GaAs, GaSb, and GaBi, as well as InP, InAs, InSb, and InBi.

IV. CONCLUSIONS

In conclusion, a plane-wave ultrasoft pseudopotential based DFT method is employed to study γ and Φ values of 12 III-V(110) surfaces. It is found that both of them have the same order of the corresponding E_c values. In terms of the above relationship between γ and E_c, the previously reported γ value of GaP(110) should be incorrect. LDA exchange-correlation functional is found to be a good one for Φ calculations. In addition, the bonding natures can be investigated by analyzing the plots of electron density difference and DOS.

ACKNOWLEDGMENTS

The authors acknowledge the financial support from National Key Basic Research and Development Program of China (Grant No. 2004CB619301), NNSFC (Grant No. 50525204), and "985 Project" of Jilin University.

*Author to whom correspondence should be addressed; FAX: +86 431 85095876; jiangq@jlu.edu.cn

[1] Ph. Ebert, Surf. Sci. Rep. **33**, 121 (1999).
[2] B. Engels, P. Richard, K. Schroeder, S. Blügel, Ph. Ebert, and K. Urban, Phys. Rev. B **58**, 7799 (1998).
[3] The 2000 Nobel Physics Prize, http://www.nobel.se/physics/laureates/2000/.
[4] S. Mirbt, N. Moll, A. Kley, and J. D. Joannopoulos, Surf. Sci. **422**, L177 (1999).
[5] W. G. Schmidt, Appl. Phys. A: Mater. Sci. Process. **75**, 89 (2002).
[6] H. M. Tütüncü and G. P. Srivastava, Phys. Rev. B **59**, 4925 (1999).
[7] H. Nienhaus, Phys. Rev. B **56**, 13194 (1997).
[8] N. Esser, K. Hinrichs, J. R. Power, W. Richter, and J. Fritsch, Phys. Rev. B **66**, 075330 (2002).
[9] H. Nienhaus and W. Mönch, Phys. Rev. B **50**, 11750 (1994).
[10] M. Ferhat and A. Zaoui, Phys. Rev. B **73**, 115107 (2006).
[11] N. Ooi and J. B. Adams, Surf. Sci. **574**, 269 (2005).
[12] W. Liu, X. Liu, W. T. Zheng, and Q. Jiang, Surf. Sci. **600**, 257 (2006), and references cited therein.
[13] V. A. Shchukin and D. Bimberg, Rev. Mod. Phys. **71**, 1125 (1999).
[14] Y. Li, G. C. Weatherly, and M. Niewczas, J. Appl. Phys. **98**, 013522 (2005).
[15] Y. Xue and M. A. Ratner, Phys. Rev. B **70**, 205416 (2004).
[16] A. Rizzi and H. Lüth, Appl. Phys. A: Mater. Sci. Process. **75**, 69 (2002).
[17] Q. Jiang, H. M. Lu, and M. Zhao, J. Phys.: Condens. Matter **16**, 521 (2004).
[18] H. L. Skriver and N. M. Rosengaard, Phys. Rev. B **46**, 7157 (1992).
[19] D. L. Price, B. R. Cooper, and J. M. Wills, Phys. Rev. B **48**, 15311 (1993).
[20] Q. Jiang, D. S. Zhao, and M. Zhao, Acta Mater. **49**, 3143 (2001).
[21] G. Renaud, Surf. Sci. Rep. **32**, 5 (1998).
[22] C. Messmer and J. C. Bilello, J. Appl. Phys. **52**, 4623 (1981).
[23] G. X. Qian, R. M. Martin, and D. J. Chadi, Phys. Rev. B **37**, 1303 (1988).
[24] N. Moll, A. Kley, E. Pehlke, and M. Scheffler, Phys. Rev. B **54**, 8844 (1996).
[25] S. B. Zhang and S. H. Wei, Phys. Rev. Lett. **92**, 086102 (2004).
[26] D. M. Ceperley and B. J. Alder, Phys. Rev. Lett. **45**, 566 (1980).
[27] J. P. Perdew and A. Zunger, Phys. Rev. B **23**, 5048 (1981).
[28] W. Liu, J. C. Li, W. T. Zheng, and Q. Jiang, Phys. Rev. B **73**, 205421 (2006).
[29] L. Vitos, A. V. Ruban, H. L. Skriver, and J. Kollár, Surf. Sci. **411**, 186 (1998).
[30] J. L. F. Da Silva, C. Stampfl, and M. Scheffler, Surf. Sci. **600**, 703 (2006).
[31] H. W. Hugosson, O. Eriksson, U. Jansson, A. V. Ruban, P. Souvatzis, and I. A. Abrikosov, Surf. Sci. **557**, 243 (2004).
[32] P. Broqvist, H. Grönbeck, and I. Panas, Surf. Sci. **554**, 262 (2004).
[33] W. Li and D. Y. Li, Chem. Phys. **122**, 064708 (2005).
[34] C. Hückstädt, S. Schmidt, S. Hüfner, F. Forster, F. Reinert, and M. Springborg, Phys. Rev. B **73**, 075409 (2006).
[35] D. Y. Li and W. Li, Appl. Phys. Lett. **79**, 4337 (2001).
[36] T. E. Fischer, Phys. Rev. **139**, A1228 (1965).
[37] T. E. Fischer, Phys. Rev. **147**, 603 (1966).
[38] G. W. Gobeli and F. G. Allen, Phys. Rev. **137**, 245 (1965).
[39] T. E. Fischer, Phys. Rev. **142**, 519 (1966).
[40] J. L. F. Da Silva, C. Stampfl, and M. Scheffler, Phys. Rev. B **72**, 075424 (2005).
[41] F. Viñes, C. Sousa, P. Liu, J. A. Rodriguez, and F. Illas, J. Chem. Phys. **122**, 174709 (2005).
[42] K. Kobayashi, Jpn. J. Appl. Phys., Part 1 **39**, 4311 (2000).
[43] K. Kobayashi, Surf. Sci. **493**, 665 (2001), and references cited therein.

[44] M. D. Segall, P. L. D. Lindan, M. J. Probert, C. J. Pickard, P. J. Hasnip, S. J. Clark, and M. C. Payne, J. Phys.: Condens. Matter **14**, 2717 (2002).
[45] D. Vanderbilt, Phys. Rev. B **41**, R7892 (1990).
[46] J. P. Perdew and Y. Wang, Phys. Rev. B **45**, 13244 (1992).
[47] S. Q. Wang and H. Q. Ye, Phys. Rev. B **66**, 235111 (2002).
[48] D. W. Palmer, http://www.semiconductors.co.uk/.
[49] W. A. Harrison, *Electronic Structure* (Freeman, San Francisco, 1980).
[50] S. Francoeur, M.-J. Seong, A. Mascarenhas, S. Tixier, M. Adamcyk, and T. Tiedje, Appl. Phys. Lett. **82**, 3874 (2003).
[51] C. Q. Sun, Prog. Solid State Chem. **35**, 1 (2007).
[52] A. E. Mattsson, P. A. Schultz, M. P. Desjarlais, T. R. Mattsson, and K. Leung, Modell. Simul. Mater. Sci. Eng. **13**, R1 (2005).
[53] D. Yu and M. Scheffler, Phys. Rev. B **70**, 155417 (2004), and references cited therein.
[54] J. C. Boettger, Phys. Rev. B **49**, 16798 (1994).
[55] D. R. Askeland and P. P. Phulé, *The Science and Engineering of Materials*, 4th ed. (Thomson Brooks/Cole, Pacific Grove, CA, 2004), p. 798.
[56] J. P. Perdew and M. Levy, Phys. Rev. Lett. **51**, 1884 (1983).
[57] M. J. Rutter and J. Robertson, Phys. Rev. B **57**, 9241 (1998).
[58] L. Ley, R. A. Pollak, F. R. McFeely, S. P. Kowalczyk, and D. A. Shirley, Phys. Rev. B **9**, 600 (1974).
[59] P. C. Rusu and G. Brocks, Phys. Rev. B **74**, 073414 (2006).
[60] C. Q. Sun, Phys. Rev. B **69**, 045105 (2004).